Modeling and Control of Propellant Slosh Dynamics in Observation Spacecraft with Actuators Saturations

Anthony Bourdelle, Jean-Marc Biannic, Burlion Laurent, Hélène Evain, Christelle Pittet, Sabine Moreno

Modeling and Control of Propellant Slosh Dynamics in Observation Spacecraft with Actuators Saturations

BOURDELLE Anthony [1†], *BIANNIC Jean-Marc* [2], *BURLION Laurent* [3]
EVAIN Helene [4], PITTET Christelle [5] and MORENO Sabine [6]
[1,2] *ONERA - The French Aerospace Lab*
2 Av. Edouard Belin, 31400, Toulouse, France
[3] *Rutgers University*
57 US Highway 1, New Brunswick, NJ 08901-8554
[4,5,6] *CNES - The French Space Agency*
18 Av. Edouard Belin, 31400, Toulouse, France
[†] Corresponding author · anthony.bourdelle@onera.fr

Abstract

In this paper, contributions to the modeling and mitigation of propellant sloshing disruptive torque, arising in particular during attitude maneuvers, are presented. The perturbation is modeled as an uncertain LPV model whose time-varying parameters are identified using CFD data. Relying on this model, the mitigation strategy consists in the design of a robust parameter-varying sloshing torque observer by means of the structured multi-model $\mathcal{H}_\infty$ framework. The estimated torque is then used to improve a satisfying attitude controller initially designed on an empty spacecraft. Finally the system reference is modified, using the *reference governor* framework, to ensure that the actuator capabilities are njot exceeded.

1. Introduction

During the acceleration phases of liquid-carrying vehicles, the on-board fluid free surface is set in motion through fluid-structure dynamical coupling. Referred to as *sloshing* [20], this low frequency and badly damped phenomenon results in disruptive forces and torques that alter the vehicle dynamics. According to the vehicle motion, various kinds of sloshing dynamics arise, for instance surface waves, bulk fluid or vortices. In the case of land and water vehicles, such as tank ships or tanker trucks, liquid surface tension effects can be neglected in front of gravity and inertial forces. This is not the case anymore in microgravity, thus surface tension has to be taken into account while considered sloshing in spacecraft. Indeed as satellites and probes carry a lifespan-defining quantity of liquid propellant consumed by thrusters to perform orbital maneuvers (station-keeping, relocation and de-orbiting), they are subject to sloshing. Therefore spacecraft experience disturbing forces and torques that affect their pointing accuracy. Spacecraft performances and stability can even be compromised due to sloshing [19], which further complicates the design of attitude controllers. Depending on the spacecraft, the on-board liquid propellant mass can be very important (cf. Table 1), resulting in large amplitude sloshing disruptive forces and torques.

Spacecraft	Mission	Engine type	Mass ratio
Dawn (2007)	Space probe	Electrical	38,6%
Astra 2A (1998)	Communications	Chemical & Electrical	36,73%
Pleiades 1A (2011)	Earth observation	Chemical	7,39%

Table 1: Comparison of the ratio between the on-board liquid mass and the launch mass

The main solution to mitigate sloshing effects is to divide propellant tanks with baffles and bladders [15, 33], which increases the sloshing frequency and reduces its amplitude, making mitigation easier. However mass is added to the spacecraft, raising mission costs. Another solution is to allow the propellant to settle down between aggressive maneuvers. This requires to introduce time margins in the mission schedule, reducing mission availability. Alternatively, instead of an usual sharp sharp bang-off-bang angular velocity reference profiles [23, 31], a smoothed reference can be considered to lower the propellant excitation. The sloshing response will then be smoother, but the whole satellite

agility may no longer be exploited. Sloshing influence can also be tempered by notch filters [28] (alone or in addition to baffles), which reduce satellites bandwidth (especially as sloshing frequencies are uncertain).

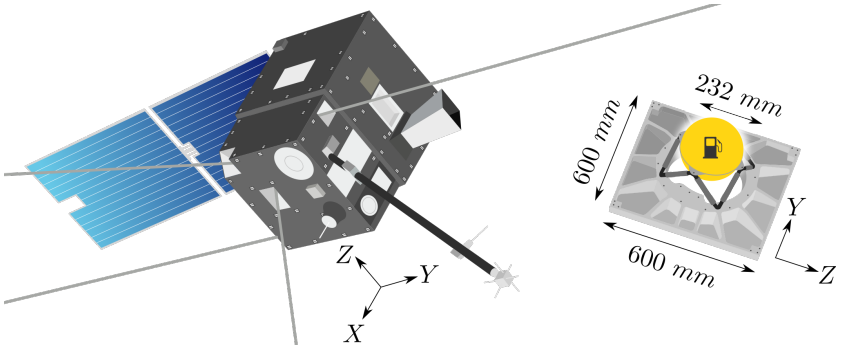

Figure 1: Illustration of a propellant tank (Demeter satellite)

From a model-based controller design perspective, the most common way to address sloshing is based on the well-known Equivalent Mechanical Models. These models approximate the liquid with a mechanical system that can be addressed like standard flexible modes [24]. Numerous models exist and reproduce a specific kind of sloshing dynamics [1, 6, 32, 36], such as spring-mass, pendulum, free-mass or mass constrained on a surface. It is of crucial important to correctly choose the mechanical parameters (such as mass, spring stiffness and pendulum length) to accurately reproduce the liquid behavior. For instance Computational Fluid Dynamics (CFD) has been used to evaluate sloshing frequencies in the *Cassini* probe tanks [17]. A Kalman filter can be used to identify a pendulum parameters [14]. The control of spacecraft with multiple propellant sloshing modes described with several pendulums has been addressed with both linear and Lyapunov-based nonlinear feedback controllers [30]. Propellant consumption can be taken into account with time-varying parameters spring-masses [18]. Uncertainties in pendulum models can be addressed with robust control [37]. Simplicity is Equivalent Mechanical Models main advantage, but it is also their main drawback. These models are based on linearized fluid dynamics models and often valid only for axisymmetric problems (e.g. hemispherical tanks accelerated along their main axis) with small amplitude motion. More importantly, they do not depend on angular speed or acceleration of the spacecraft, which however induce significant large inertial forces acting on the fluid.

Infinite-dimensional models can also be used to represent sloshing with partial differential equations and can be used to write three-dimensional sloshing equations for prescribed motion of tanks [5], to consider direct actuation of tank speed or acceleration [26] or to use the Port-Hamiltonian formalism [16] to design a controller for slosh mitigation in a fluid-coupled structure [12]. However most of time simplified infinite-dimensional sloshing models are considered, generally shallow waters equation, which are valid only for low filling ratio, perfect fluid and negligible tension surface effects. The generalization to Navier-Stokes equations with terms accounting for inertial forces and tension surface, which represent the most accurate description of sloshing, is very complex. Far from the Attitude and Orbit Control Systems paradigm, this complexity prohibits the use of controller design and stability analysis tools.

Midway between equivalent mechanical and infinite-dimensional models, Smooth Particle Hydrodynamics [35] is an interesting alternative to model fluids. It is a meshless Lagrangian method in which fluids are divided in discrete elements, called particles, that are individually followed. Based on a spatial discretization of partial differential equations, the continuity of fluid properties is obtained by kernel interpolation. The contribution of each particle is weighted by the distance to the point of measure and a kernel function (e.g. gaussian) determines how measures will be smoothed. Surface tension and wetting effects can be taken into account [11]. This method is widely used in realistic fluid simulation for video games or cinematography. To be physically accurate a high number of particles (at least several hundred for a small tank) have to be used, resulting in a high dimension model and heavy calculations, and limit conditions (interaction with tank walls) can be uneasy to implement. Suitable for validation and simulations, the computational burden is still to heavy to be used for attitude controller design.

Very effective Attitude Control Systems (ACS) are mandatory to ensure more and more stringent attitude pointing accuracy and stability requirements. Thus sloshing dynamics models have to become more reliable, for both fast simulations and controller design. Following recent progress in Computational Fluid Dynamics, the fluid behavior in maneuvering spacecraft can now be accurately computed [22, 34]. Inspired by equivalent mechanical models, we

previously proposed a reformulation of the slosh effects as an uncertain Linear Parameter Varying (LPV) model [9] whose parameters identification is supported by CFD-data [10]. A robust LPV state observer is then designed to compute a reliable estimate of the sloshing torque despite model uncertainties, in order to to decouple the satellite and sloshing sloshing dynamics, and ensure an accurate attitude control with reduced settling time [10].

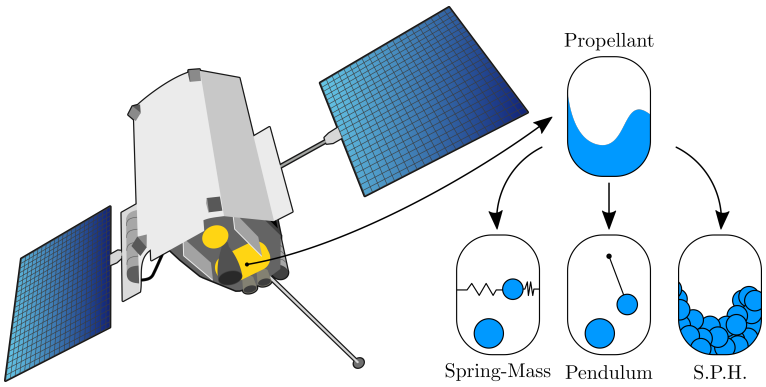

Figure 2: Illustration of Equivalents Mechanicals Models and Smooth Particle Hydrodynamics (Messenger probe)

Small satellites attitude control system generally relies on reaction wheels to provide the torque necessary to perform the desired maneuver. When the wheel angular velocity changes, the spacecraft rotates proportionally according to the conservation of angular momentum. As they are electrically powered, propellant can be saved for orbit control. However, reaction wheels have a maximum torque capability and they end up to store enough momentum to reach angular speed saturation. Other actuators, such as magnetorquers, are required to evacuate the surplus of angular momentum. It is of crucial importance to not exceed the reaction wheels torque and momentum capabilities during a maneuver, at the risk of jeopardizing the mission. For this purpose, the reference that has to be followed by the parameter-varying system is modified, in order to ensure maximum torque and momentum constraints, according to a *reference governors* [21] inspired computation.

This paper is organized as follows. Section 2 outlines our innovative slosh model and the related CFD data based identification procedure, the uncertain LPV model of the propellant-filled satellite is then introduced. The aforementioned robust sloshing torque observer design is presented in section 3. Next, section 4 provides simulations results arising from the time-varying implementation of our observer-based enhanced attitude control along with a stability and robustness analysis. A *reference governor* inspired procedure is detailed in section 5, resulting in an sloshing torque compensation scheme able to deal with sloshing despite actuators saturations. Finally, concluding comments and perspectives are proposed in section 6.

2. Nonlinear sloshing torque dynamics model

Nowadays several Computational Fluid Dynamics solvers [22, 34], supported by experiments in space (such as SloshSat-FLEVO [29] and Fluidics [25]), are able to accurately compute sloshing phenomenon in spacecraft during attitude maneuvers. In this section we consider a satellite performing attitude maneuver around a single axis, though the subsequent development can be generalized to three-axis maneuvers.

2.1 Sloshing torque modeling

Sloshing dynamics depends on :

- tank filling ratio (quantity of propellant)
- gravitational acceleration effects
- propellant properties, e.g. density, surface tension
- tank geometry (baffles, bladders etc.) and position inside the spacecraft (linked to inertial forces)
- spacecraft angular velocity and acceleration (linked to inertial forces)

Electrical powered actuators, such as reactions wheels or control moment gyros, are preferred for attitude control (propellant is saved to perform orbit control with thrusters) which results in a constant tank filling ratio. As we are considering a spacecraft attitude maneuver in microgravity, we assume that gravitational effects are negligible in front of inertial and surface tension effects. Also, the tank is considered rigid and its position fixed inside the spacecraft. Hence, only the dependence to the angular velocity $\Omega(t)$ and acceleration $\dot{\Omega}(t)$ have to be taken into account by the sloshing torque model. For clarity reasons, the time-dependence will be omitted in the next equations.

In order to get an accurate model of the propellant sloshing-spacecraft dynamical interaction, we previously proposed [10] to describe the sloshing torque Γ_F as the output of a nonlinear second order system with varying frequency ω and damping ratio ξ that are functions of spacecraft angular velocity and acceleration :

$$\ddot{\Gamma}_F + C_s(\Omega,\dot{\Omega})\dot{\Gamma}_F + K_s(\Omega,\dot{\Omega})\Gamma_F = -A_s(\Omega,\dot{\Omega})\Omega - B_s(\Omega,\dot{\Omega})\dot{\Omega} \quad (1)$$

$$C_s(\Omega,\dot{\Omega}) = 2\xi(\Omega,\dot{\Omega})\omega(\Omega,\dot{\Omega}) \quad (2)$$

$$K_s(\Omega,\dot{\Omega}) = \omega(\Omega,\dot{\Omega})^2 \quad (3)$$

As equation 1 is very similar to the standard representation of Linear Time Invariant flexible modes, we can consider this nonlinear model as a generalization equivalent mechanical models. Note that the nonlinear properties of this model result from the dependence of A_S, B_S, C_S and K_S to $(\Omega,\dot{\Omega})$ that can be identified by using numerically computed sloshing torque data.

2.2 CFD data based identification procedure

Without a prori idea of the model parameters dependency to the angular velocity and acceleration, we are in a so-called black-box case. We can capture some of the sloshing dynamics nonlinearities by making the identification on a set of N small time intervals on which both Ω and $\dot{\Omega}$ are assumed constant and the nonlinear model becomes Linear Time Invariant (LTI). By doing so we average the parameters (and indirectly the nonlinearities) on these intervals to get the evolution of the parameters. As a result we get N sets $\{C_{s_i}, K_{s_i}, A_{s_i}, B_{s_i}\}_{i\leq N}$ associated to $\{\Omega_i, \dot{\Omega}_i\}_{i\leq N}$. Using CFD data, it is possible to get boundaries for sloshing frequency and damping ratio in order to constrain C_S and K_S as described by equations (2) and (3). This identification procedure has been successfully applied [10] using constrained least squares method on DIVA data sets courtesy of *Institut de Mécanique des Fluides de Toulouse*. Standard curve-fitting techniques may then be used to rewrite each parameters as multivariate polynomials of Ω and $\dot{\Omega}$, for example. However it is not necessary to get explicit functions in order to design a sloshing torque observer, as detailed in section 3.

2.3 Propellant-filled satellite as an uncertain LPV model

From Equation (1), a state-space representation of the sloshing torque is readily deduced :

$$\underbrace{\begin{pmatrix}\dot{\Gamma}_F\\ \ddot{\Gamma}_F\end{pmatrix}}_{\dot{x}_F} = \underbrace{\begin{pmatrix}0 & 1\\ -K_S(\Omega,\dot{\Omega}) & -C_S(\Omega,\dot{\Omega})\end{pmatrix}}_{A_F(K_S,C_S)}\underbrace{\begin{pmatrix}\Gamma_F\\ \dot{\Gamma}_F\end{pmatrix}}_{x_F} + \underbrace{\begin{pmatrix}0 & 0\\ -A_S(\Omega,\dot{\Omega}) & -B_S(\Omega,\dot{\Omega})\end{pmatrix}}_{B_F(A_S,B_S)}\begin{pmatrix}\Omega\\ \dot{\Omega}\end{pmatrix} \quad (4)$$

$$\Gamma_F = \begin{pmatrix}0 & 1\end{pmatrix}x_F \quad (5)$$

For the sake of clarity, the dependencies to $(\Omega,\dot{\Omega})$ will be omitted thereafter. The parameters A_S, B_S, C_S and K_S are affected by uncertainties, which arise from numerical simulations, identification and modeling errors. These uncertainties are poorly known, thus the development of any accurate model (based on the Linear Fractional Transformation for instance) is not going to benefit to the observer design. Instead, a bounded disturbance w that bear the aforementioned uncertainties is introduced, such that $\|w\|_2 \leq \overline{w}$. Equation 4 thus becomes :

$$\dot{x}_F = A_F(K_S,C_S)x_F + B_F(A_S,B_S)\begin{pmatrix}\Omega\\ \dot{\Omega}\end{pmatrix} + \begin{pmatrix}0\\ 1\end{pmatrix}w \quad (6)$$

Let us consider the LTI state-space representation of the single-axis dynamics of an actuated satellite :

$$\dot{x}_{SAT} = A_{SAT}x_{SAT} + B_{SAT}(\Gamma_F + \Gamma_P + \Gamma_C) \quad (7)$$

$$\theta = C_\theta x_{SAT} \quad (8)$$

where Γ_P is a non-sloshing disturbing torque, Γ_C is the control torque and θ is the satellite attitude.

In order to also estimate Γ_P, we extend the state vector and, without any information, we consider it constant :

$$\dot{\Gamma}_P = 0 \tag{9}$$

The identification results highlight that the parameters B_S and C_S can be approximated by linear functions respectively of A_S and K_S :

$$B_S = \alpha_{AB} A_S + \beta_{AB} \tag{10}$$
$$C_S = \alpha_{KC} K_S + \beta_{KC} \tag{11}$$

Combining Equations (5)-(11), the propellant-filled satellite dynamics with its actuators can be described by the following uncertain LPV system :

$$\dot{x} = A(\alpha(t))x + B_u \Gamma_C + \underbrace{[0\ 1\ 0\ \dots\ 0]^T}_{B_w} w \tag{12}$$

$$\begin{pmatrix} \theta \\ \Gamma_D \end{pmatrix} = \begin{bmatrix} C_m & C_z \end{bmatrix}^T x \tag{13}$$

where :

$$\alpha(t) = (\alpha_A(t), \alpha_K(t))$$
$$= (A_S[\Omega(t), \dot{\Omega}(t)], K_S[\Omega(t), \dot{\Omega}(t)]) \tag{14}$$
$$\Gamma_D = \Gamma_F + \Gamma_P \tag{15}$$
$$x = [x_F\ x_{SAT}\ \Gamma_P]^T \tag{16}$$

Due to the action of the Attitude Control System, and the reaction wheels limited actuation capabilities, we can consider restricted variations of $(\Omega(t), \dot{\Omega}(t))$:

$$|\Omega(t)| \leq S_C \bar{\Omega} \tag{17}$$
$$|\dot{\Omega}(t)| \leq S_C \bar{\dot{\Omega}} \tag{18}$$

where $\bar{\Omega}$ and $\bar{\dot{\Omega}}$ are the spacecraft maneuver capabilities, and S_c a security coefficient (equal to 1.5 for this study). This permits to characterize a narrowed definition domain for A_S and K_S. Thus, the time-varying vector $\alpha(t)$ takes its values in a polytope $\mathcal{P}$ of 15 vertices $\mathcal{P}_i,\ i \in \{1, 2, \dots, 15\}$:

$$\alpha(t) \in \mathcal{P} := Co\{\mathcal{P}_1, \mathcal{P}_2, \dots, \mathcal{P}_9\} \tag{19}$$

Remark. *Due to the filtering effect of the actuators, the parametric variations appear only in the A matrix of the state-space representation. Note that the use of α as the system parameter, instead of $(\Omega, \dot{\Omega})$, has the following advantages :*

- *$A(\alpha)$ is a linear function of α which will simplify both the observer design and stability analysis,*
- *A_S, B_S, C_S and K_S do not need to be explicitly written as functions of $(\Omega, \dot{\Omega})$*

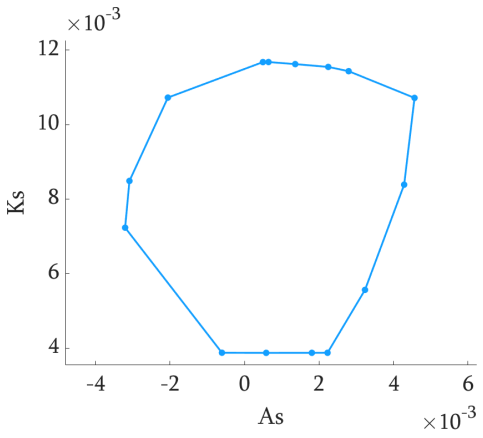

Figure 3: $\alpha(t)$ parameter polytope $\mathcal{P}$

3. Robust $\mathcal{H}_\infty$ based observer design with parameter-varying gain

The uncertain LPV model of the propellant-filled satellite, described by the state-space representation given by Equations (12) and (13), is now used to design a sloshing torque observer robust to model uncertainties by using the structured multi-model $\mathcal{H}_\infty$ framework.

3.1 Problem statement

The objective is to enhance the performances of any existing controller that has been design without considering sloshing. In order to achieve an efficient sloshing mitigation, the estimated of disturbing torques is used to decouple the satellite from the sloshing dynamics and other perturbations. An LPV observer has then to be designed in order to provide a reliable estimation of the disturbing torque than can next be easily canceled from the control input. Such an observer is described by :

$$\begin{aligned}
\dot{\hat{x}} &= A(\alpha(t))\hat{x} + B_u\Gamma_C + L(\alpha(t))(\theta - \hat{\theta}) && (20)\\
&= \underbrace{(A(\alpha) - L(\alpha)C_m)}_{A_{Obs}}\hat{x} + \underbrace{[B_u \quad L(\alpha)]}_{B_{Obs}}[\Gamma_C \quad \theta]^T && (21)\\
\hat{\Gamma}_D &= C_z x + \underbrace{[0 \quad 0]}_{D_{Obs}}[\Gamma_C \quad \theta]^T && (22)
\end{aligned}$$

where $\hat{x}$ and $\hat{\Gamma}_D$ are the estimates of respectively x and Γ_D, and $L(\alpha)$ is the observer gain that has to be designed. The dynamics of the state error is represented by the system :

$$(\mathcal{S})\begin{cases}
\dot{\epsilon} = A_{Obs}x + B_w w,\ \epsilon = x - \hat{x} & (23)\\
z = C_z\epsilon & (24)\\
\quad = \Gamma_D - \hat{\Gamma}_D & (25)
\end{cases}$$

To ensure an efficient compensation, the estimated disruptive torque needs to be accurate despite model disturbances w. It should also take into account the fact that the compensation is realized by actuators whose dynamics introduce rather small but not negligible delays. As is clarified next, this can be achieved by the introduction of a small derivative term in the signal to be estimated.

Remark. *The different state-space representations that have been introduced so far, in particular Equations (20) and (23), do not depend at all of a given controller, but only on the torque Γ_C applied to the system. This means that the observer based compensation scheme is independent from any controller, thus this method can be straightforwardly implemented in any system.*

3.2 Tuning process and resolution aspects

As previously noted, the choice of the parameter α implies that the $A(\alpha)$ matrix in the state-space representation given by Equation (23) is a linear function of α. Thus we can write :

$$A(\alpha) = A_0 + \alpha_A A_A + \alpha_K A_K \tag{26}$$

We then propose to search a structured observer gain that mimics the $A(\alpha)$ matrix :

$$L(\alpha) = L_0 + \alpha_A L_A + \alpha_K L_K \tag{27}$$

The system $(\mathcal{S})$ has an affine LPV structure given by (26), hence a polytopic model on $\mathcal{P}$ can be easily deduced :

$$\begin{aligned}
\alpha &= \sum_{i=1}^{15}\beta_i\mathcal{P}_i && (28)\\
\mathcal{S}(\alpha) &= \sum_{i=1}^{15}\beta_i\mathcal{S}(\mathcal{P}_i) && (29)
\end{aligned}$$

where :

$$\beta_i \geq 0 \tag{30}$$

$$\sum_{i=1}^{15} \beta_i = 1 \tag{31}$$

As stated by [7], this approach is suitable to be addressed by a $\mathcal{H}_\infty$ multi-model robust design techniques on the 15 LTI models ($S_{i\leq 15}$), that corresponds to the LPV system frozen at the vertices $\mathcal{P}_{i\leq 15}$. The problem is then to compute the matrices L_0, L_A and L_K of the observer parameter-varying gain such that the error dynamics (and therefore the observer dynamics) is quadratically stable over $\mathcal{P}$ and $\|z\|_2 < \|w\|_2$ to ensure robustness to model uncertainties.

The flexibility of nonsmooth optimization algorithms implemented in the `systune` routine of the Matlab^{TM} Robust Control Toolbox (see [3, 4]) allows the computation of bounded gains L_0, L_A and L_K so as to minimize the estimation error z as further detailed and to constrain the observer/error dynamics. For implementation purposes, the following constraints have been defined :

- Minimum decay rate : 0.001 rad/s, to ensure a non-marginal stability
- Minimum damping ratio : 0.7, to ensure a satisfying damping of the estimation error
- Maximum observer frequency : 10 rad/s, to avoid too fast oscillations
- Absolute value of gains < 2, to reduce noise sensitivity

Actuator low-pass dynamics compensation is achieved by introducing a derivative term in the estimated torque z :

$$z = (\Gamma_D - \hat{\Gamma}_D) + E(\dot{\Gamma}_F - \dot{\hat{\Gamma}}_F) \tag{32}$$

where the gain E is tuned according to the characteristics of the actuator.

In order to minimize the steady-state estimated torque error, while not being too restrictive during the optimization, the error signal z and the model uncertainties w are weighted respectively by a low-pass transfer function $W_z(s)$ and a constant filter $W_w(s)$:

$$W_z(s) = W_{z,0}\frac{0.1}{s+0.1},\ W_{z,0} = 2.79 \tag{33}$$

$$W_w(s) = 0.01 \tag{34}$$

The filter $W_z(s)$ is designed such that the transfer between the model disturbance w and the output z is as small as possible given the observer gains constraints, mainly in low-frequency (assuming that the model disturbance is a low-frequency signal). The filter $W_w(s)$ is equal to the maximum amplitude of w and it calibrates the input signal. Note that the value 0.01 is almost ten times higher than the sloshing torque maximum amplitude, which ensures an effective rejection of the model disturbance.

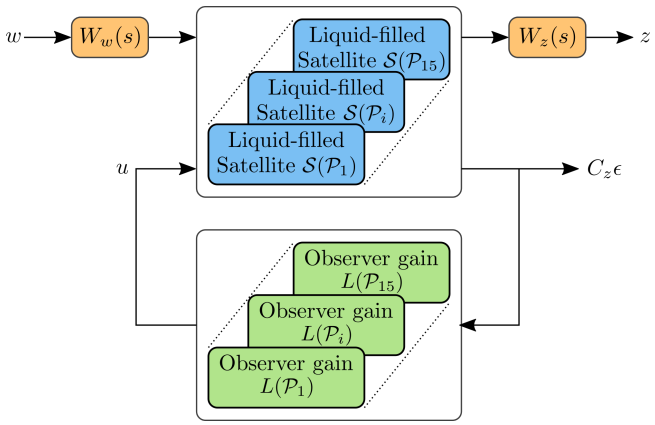

Figure 4: Design model block diagram

4. Results, stability and robustness analysis

The required attitude control performances are inspired by [27], that provides a benchmark corresponding to the *Demeter* satellite bus :

- Pointing steady-state error < 0.04 deg
- Pointing rate steady-state error < 0.1 deg/s
- Angular momentum < 0.12 Nms
- Control torque < 0.005 Nm

We consider a satellite with an inertia $I_z = 30$ kg.m^2 corresponding to the *Demeter* satellite, whose attitude is controlled by the following Proportional-Derivative controller such that performances criteria are respected in the absence of sloshing :

$$\Gamma_C = \underbrace{0.3553}_{K_P}\delta_\theta + \underbrace{6.2845}_{K_D}\delta_\Omega \tag{35}$$

where δ_θ is the attitude error and δ_Ω is the angular velocity error.

Remark. *The Attitude Control System in the Demeter benchmark computes the velocity is pseudo-derived from the attitude measurement provided by a star tracker. Here, angular velocity is provided by adding an output to the observer.*

The actuator is a reaction wheel whose low-pass dynamics is modeled by the following transfer function :

$$RWS(s) = \frac{1.2s + 0.76}{s^2 + 2.4s + 0.76} \tag{36}$$

To get faster responses we also add the torque guidance profile Γ_d in a feed-forward path.

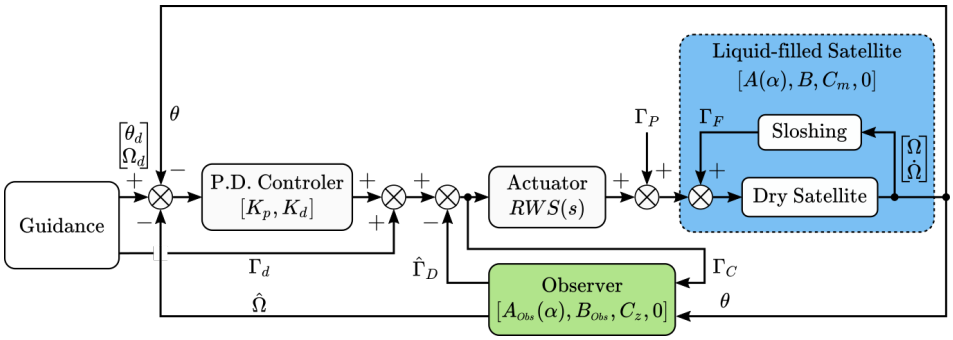

Figure 5: Parameter-varying closed-loop model block diagram

4.1 Observer and global closed-loop plant stability analysis

The multi-model $\mathcal{H}_\infty$ based approach, based on LTI design tools, offers great flexibility in the design of the observer, however there is no theoretical guarantee regarding time-varying stability. The latter should then be checked *a posteriori*. This is achieved here with the help of quadratic Lyapunov functions for both the observer and the global closed-loop plant.

Observer stability : We focus beforehand on the stability analysis of the parameter-varying observer dynamics. This is easily verified, independently of the rate of variation of the parameters, if a symmetric positive definite matrix $P_{Obs} > 0$, associated to the quadratic Lyapunov function $V(x) = x^T P_{Obs}\, x$, can be found such that :

$$A_{Obs}(\alpha)^T P_{Obs} + P_{Obs} A_{Obs}(\alpha) < 0,\ \forall \alpha \in \mathcal{P} \tag{37}$$

Using the polytopic model given by Equations (28) and (29), it reduces to 15 Linear Matrix Inequalities (LMI) :

$$A_{Obs}(\mathcal{P}_i)^T P_{Obs} + P_{Obs} A_{Obs}(\mathcal{P}_i) < 0, \quad i = 1, \ldots, 15 \tag{38}$$

Since the observer has 7 states, the above LMI problem exhibits $7 \times 8/2 = 28$ decision variables and was easily solved using the standard `feasp` LMI solver available with the Matlab Robust Control Toolbox. It can then be concluded that the observer remains stable for arbitrarily fast variations of the parameters inside the polytope $\mathcal{P}$.

Global closed-loop plant stability : Let us now focus on the parameter-varying closed-loop plant. As it results from a linear interconnexion of LTI and LPV systems that affinely depends on α, the closed-loop dynamics is described by a matrix $A_{CL}(\alpha) \in \mathbb{R}^{13\times13}$ with the same properties. Thus $A_{CL}(\alpha) \in Co\{A_{CL}(\mathcal{P}_1), \ldots, A_{CL}(\mathcal{P}_9)\}$. The stability analysis of the closed-loop dynamics follows the same strategy than the observer stability analysis. Since the closed-loop has 13 states, the LMI problem now exhibits $13 \times 14/2 = 91$ decision variables. As the problem has been solved, we can conclude that the closed-loop with sloshing torque compensation remains stable for arbitrarily fast variations of the parameters inside the polytope $\mathcal{P}$.

Remark. *When the security coefficient S_C exceeds a threshold value, quadratic stability cannot be proved anymore. A Parameter-Dependent Lyapunov Function $P(\alpha)$ allowing to take into account bounds on the rate of variation of the parameters $\alpha_A = A_S$ and $\alpha_K = K_S$ needs to be considered. The following polynomial form is suggested :*

$$\begin{aligned} P(\alpha) = P_0 + \alpha_A P_A + \alpha_K P_K + \alpha_A\alpha_K P_{AK} \\ + \alpha_A^2 P_{A_2} + \alpha_K^2 P_{K_2} \end{aligned} \tag{39}$$

Assuming that $|\dot{\alpha}_A| < \rho_A$ and $|\dot{\alpha}_K| < \rho_K$, new stability conditions are obtained as, $\forall\alpha \in \mathcal{P}$:

$$\begin{aligned} A_{CL}(\alpha)^T P(\alpha) + P(\alpha)A_{CL}(\alpha) \\ \pm \rho_A(P_A + \alpha_K P_{AK} + 2\alpha_A P_{A_2}) \\ \pm \rho_K(P_K + \alpha_A P_{AK} + 2\alpha_K P_{K_2}) < 0 \end{aligned} \tag{40}$$

$$P(\alpha) > 0 \tag{41}$$

In the above conditions, the first inequality is now a nonlinear function (second-order polynomial) of the parameters. Different techniques exist to transform the above problem into a finite set of LMIs. The less conservative approach consists of searching for $P_0, P_A, \ldots, P_{K_2}$ on a given grid and then to check a posteriori whether $P(\alpha)$ satisfies the constraints everywhere inside the polytope. As shown in [8] this test can be performed almost non conservatively by computing μ upper and lower bounds if the parameters are independent. If it is not the case, the grid has to be dense enough so that an argument of continuity is applicable.

In our case, an initial grid with 24 *points taken over the polytope $\mathcal{P}$ has been defined. Then a total number of* $5 \times 24 = 420$ *LMIs was considered with* $6 \times 13 \times 14/2 = 546$ *decision variables. For realistic bounds $\rho_A = 5.6 \times 10^{-4}$ and $\rho_K = 2.5 \times 10^{-3}$ (induced by extremal values of Ω and $\dot{\Omega}$ taken from intensive simulations), a solution was found and validated by on a very dense grid of* 190000 *points in a reasonable time (less than 3 min) on a standard computer.*

4.2 Simulation results

The parameter-varying observer performances are compared to two alternative observers whose design is also based on a $\mathcal{H}_\infty$ multi-model design technique with the same constraints and filter $W_w(s)$. The first observer has a fixed gain, while the second one was based on a rigid satellite model that does not take sloshing into account and assumes that $\dot{\Gamma}_D = 0$, as we did for Γ_P. The value of $W_{z,0}$ in the filter $W_z(s)$ is taken such that the $\mathcal{H}_\infty$ norm of the weighted transfer from w to z is equal to 1. Thus $W_{z,0} = 2.41$ for the fixed gain observer and $W_{z,0} = 99$ for the rigid model observer.

Remark. *The* `Simulink` *model used for the simulations does not consider the linear approximations given by Equations (11) and (10) but the complete set of parameters $\{A_S, B_S, C_S, K_S\}$ from the identification, hence the parameters used by the observers and the ones used by the sloshing torque model are slightly different.*

Figures 6 to 8 present simulation results, that compare observers performances on the velocity and attitude reference tracking and the estimation of the disturbing torque, for a slightly smoothed bang-off-bang reference profile. Note that the initial sloshing torque is $\Gamma_{F,0} = -0.0027$ Nm, and that the torque error is obtained by making the difference between the actual torque and the torque estimate filtered by the actuator.

Those results confirm that a better tracking is achieved by using a sloshing torque observer. Despite the limiting constraints of the design procedure, both parameter-varying gain and fixed gain observer efficiently estimate the disruptive torque and allow a very satisfying compensation. Figure 7 reveals that in the case of an effective compensation, the attitude error requirement is respected sooner and for a longer time. The rigid model performances are quite poor and even worse than the single action of the proportional-derivative controller. Note that the angular velocity error is ensured by every compensation scheme. The performances of the parameter-varying gain and fixed gain observer are closely similar. However the parameter-varying gain observer achieve better robustness performances, its value of $W_{z,0}$ and value of S_C (at which quadratic stability is lost) are higher than the ones of the fixed gain observer.

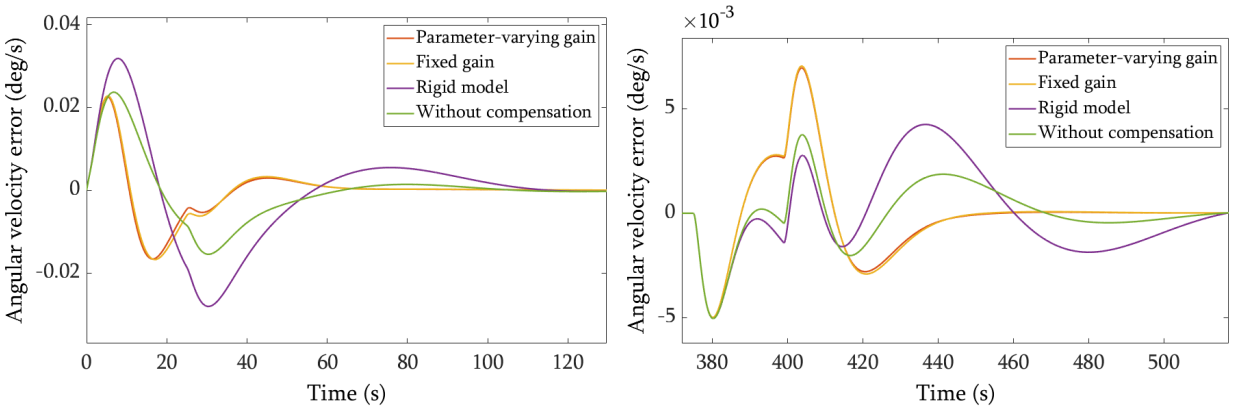

(a) Velocity rise (b) Velocity fall

Figure 6: Observers performances comparison - Angular velocity error

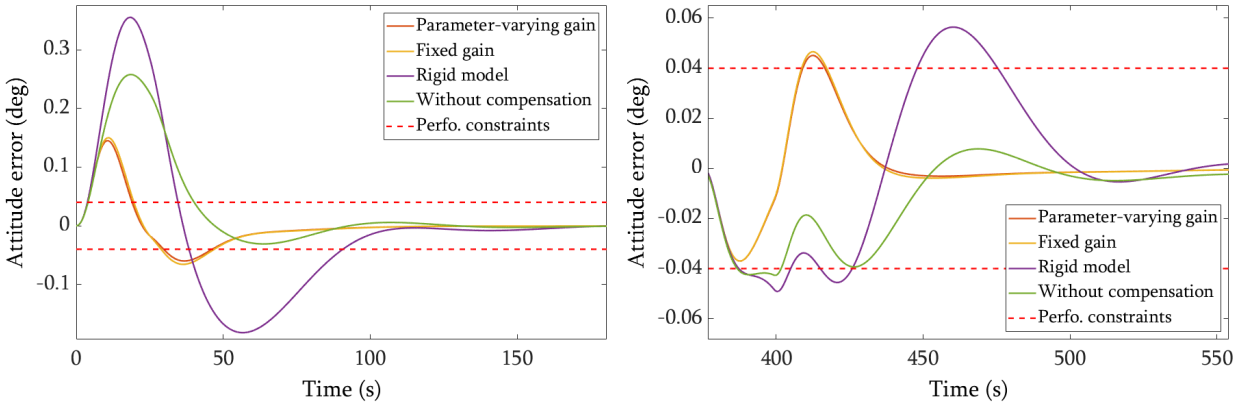

(a) Attitude rise (b) Attitude level

Figure 7: Observers performances comparison - Attitude error

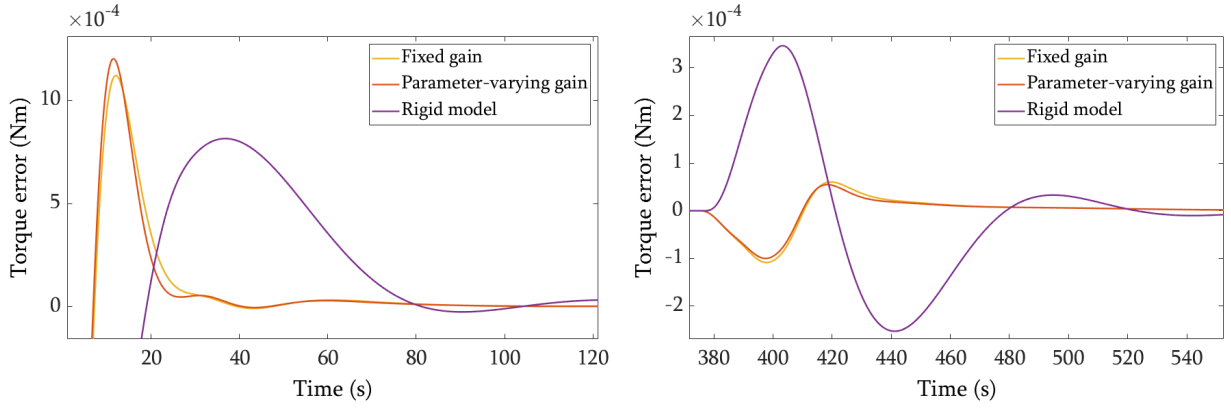

(a) First *bang* (b) Second *bang*

Figure 8: Observers performances comparison - Estimated torque error

4.3 Robustness to parameters uncertainties analysis

During the observer design it was assumed that the value of the parameter $\alpha(t)$ is the same for both the observer and the sloshing torque model. However this will not be the case during the compensation scheme implementation, as only an estimated value of $\alpha(t)$ will be provided to the observer. It is then necessary to verify that the sloshing torque estimate

is still reliable when we consider a parameter $\alpha(t)$ for the sloshing torque model and a different parameter $\alpha_{Obs}(t)$ for the observer. To do so we introduce parameter perturbations $\Delta_A(t)$ and $\Delta_K(t)$ such that :

$$\alpha_{A,Obs}(t) = \alpha_A(t)\,[1 + \Delta_A(t)] \quad (42)$$
$$\alpha_{K,Obs}(t) = \alpha_K(t)\,[1 + \Delta_A(t)] \quad (43)$$

The objective is then to evaluate in which domain $\{\Delta_A(t), \Delta_K(t)\}$ can evolve without compromising the system stability and performances. It has been attempted to prove the stability by using parameter dependent Lyapunov functions, however it appeared that the subsequent LMI problem are marginally unfeasible, simulations suggest that it is a consequence of numerical errors or that this approach is still too conservative. Indeed, simulation results analysis for $(|\Delta_A(t)|, |\Delta_K(t)|) \in [-0.9, 0.9]\times[-0.9, 0.9]$ exhibit an effective handling of parameters perturbations without any loss of stability. Figure 9 compares the performances of the system with the nominal α parameter and the system whose parameter α parameter is disrupted by $\Delta_A(t) = 0.9\sin(0.05t)$ and $\Delta_K(t) = -0.9\sin(0.02t)$. It highlight a slightly, but acceptable, degradation of the performances when the parameter $\alpha(t)$ is disrupted.

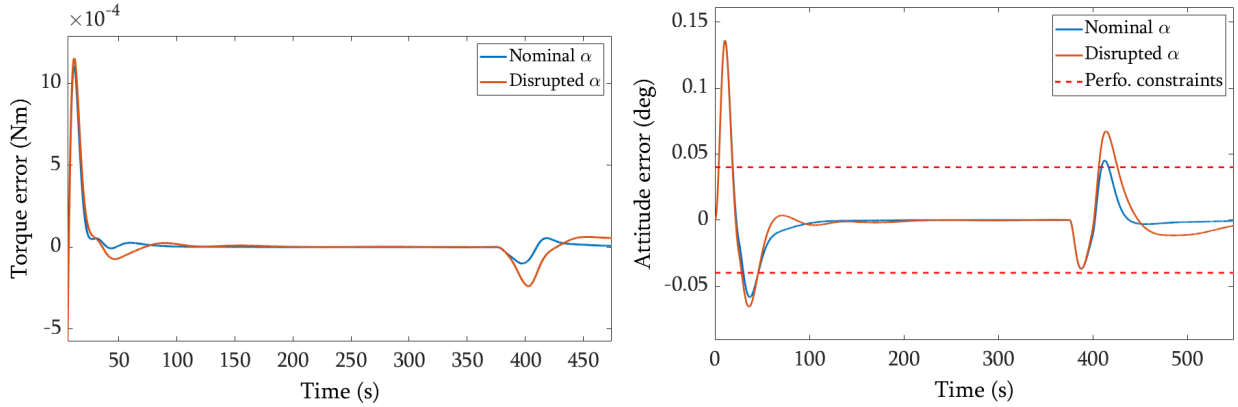

(a) Estimated torque

(b) Attitude error

Figure 9: Parameters perturbations rejection performances

5. Reference adaptation to address actuators saturations

Depending on the initial conditions $\Gamma_{F,0}$, actuators capabilities may reach torque and momentum saturations, as illustrated by Figure 10. Since these strong nonlinearities are not taken into account in the observer design model, it can lead the system to instability. To avoid these saturations, an adaptation of the reference given by the guidance system is proposed. It relies on the *reference governors* framework [21] to ensure the respect of actuators capabilities.

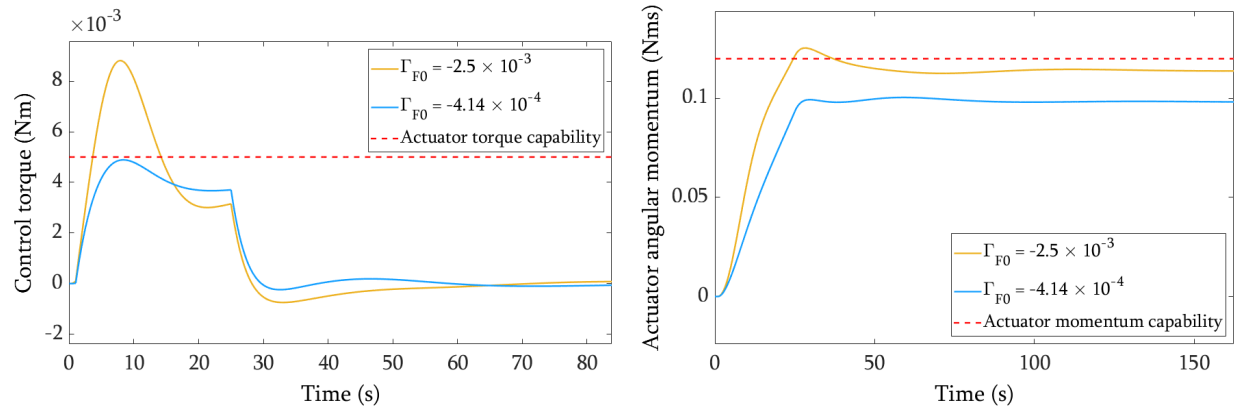

(a) Control torque

(b) Angular momentum

Figure 10: Control torque and angular momentum in function of the initial condition

5.1 Reference governors inspired procedure

Inspired by the design of reference governors for nonlinear system embedded into a LPV system (cf. [2, 13]) we propose a practical and easily implementable reference governor design for the global closed-loop plant.

Let us consider the discrete state-space representation of the closed-loop system for a given time step dT, small enough so that the discretization preserves the system dynamics properties :

$$\begin{aligned} x(k+1) &= A^d_{CL}(\alpha(k))x(k) + B^d_{CL}u(k),\ \forall k \in \mathbb{N} && (44)\\ y_{RG}(k) &= C^d_{CL}x(k) + D^d_{CL}u(k) && (45)\\ &= [\Gamma_C(k), H_w(k)]^T && (46)\\ u(k) &= K_P\theta_d + K_D\Omega_d + \Gamma_d && (47) \end{aligned}$$

where u is the reference, given in terms of the angular velocity Ω_d, torque Γ_d and attitude θ_d guidance profile references, Γ_C is the control torque and H_w is the actuator angular momentum. The objective is to find at each instant a reference $v(k)$, as close as possible from $u(k)$, which ensures the following constraints, $\forall k \in \mathbb{N}$:

$$-\bar{\Gamma}_C \leq \Gamma_C(k) \leq \bar{\Gamma}_C \quad (48)$$

$$-\bar{H}_w \leq H_w(k) \leq \bar{H}_w \quad (49)$$

As stated in [21], *reference governor* schemes usually compute a constant reference v_0 such that if $v(k) = v_0, \forall k \in \mathbb{N}$, the output $y_{RG}(k)$ always satisfy the constraints, which guarantee a constraint enforcement safety. In the context of this article, the parameter α is slowly varying, so that it is possible to consider it constant for a short horizon of time $[k, k+h], h \in \mathbb{N}$. Consequently we propose to use a finite horizon to compute v_0, rather that an infinite horizon. Note that is will ease the implementation of the *reference governor* scheme and reduce computational burden. By considering $v(i) = v_0, \forall i \in [k, k+h]$ as system input instead of u and a frozen parameter $\alpha(k)$, Equations (44) and (45) become :

$$\begin{aligned} x(i+1) &= A^d_{CL}(\alpha(k))x(i) + B^d_{CL}v_0,\ \forall i \in [k, k+h] && (50)\\ y_{RG}(i) &= C^d_{CL}x(i) + D^d_{CL}v_0 && (51) \end{aligned}$$

The system given by Equation (50) and (51) is then Linear Time Invariant, thus we can write:

$$\begin{aligned} x(i+1) &= A^d_{CL}(\alpha(k))^(i-k+1)x(k) + B^d_{CL}v_0,\ \forall i \in [k, k+h] && (52)\\ y_{RG}(i) &= \begin{bmatrix} C^d_{CL} & D^d_{CL} \end{bmatrix} \Phi^(i-k+1) \begin{bmatrix} x(k) \\ v_0 \end{bmatrix} && (53)\\ \Phi &= \begin{bmatrix} A^d_{CL}(\alpha(k)) & B^d_{CL} \\ 0 & I \end{bmatrix} && (54) \end{aligned}$$

Using Equations (52) to (54), Equations (48) and (49) become :

$$\begin{bmatrix} C^d_{CL} & D^d_{CL} \\ -C^d_{CL} & -D^d_{CL} \end{bmatrix} \Phi^(i-k+1) \begin{bmatrix} x(k) \\ v_0 \end{bmatrix} \leq \begin{bmatrix} \bar{\Gamma}_C \\ \bar{\Gamma}_C \\ \bar{H}_w \\ \bar{H}_w \end{bmatrix},\ \forall i \in [k, k+h] \quad (55)$$

The computation of v_0 at instant k reduces to solving the following optimization problem :

$$\begin{aligned} \underset{v_0}{\text{minimize}} \quad & d(v_0, u(k)) \\ \text{subject to} \quad & Eq.\,(55) \end{aligned} \quad (56)$$

where $d(v_0, u(k))$ denotes the Euclidean distance between v_0 and $u(k)$.

5.2 Implementation

This *reference governor* simplified procedure requires to correctly chose the time horizon length h so that a solution v_0 to the optimization problem (56) exists. An algorithm is proposed in [2], however a more practical and direct

approach has been considered, yet it propose less theoretical guarantees. The time horizon length h is chosen so that the hypothesis of a constant $\alpha(k)$ parameter holds, if no solution to the optimization problem is found, then h is reduced by one until a solution is found. During the implementation a value $h = 120$ has been satisfying with no occurrence of an absence of solution. The optimization problem has been solved by using the `lsqlin` routine in Matlab, which is able to solve constrained linear least-squares problems. During implementation the discrete state-space representation has been computed using a Tustin approximation by means of `c2d` Matlab routine with a sample time $dT = 0.025$ s.

5.3 Simulation results

Figure 11 compare the system behavior with and without *reference governor*. Despite adverse initial conditions, that lead to the violation of both control torque and actuator angular momentum constraints, the system enhanced by a *reference governor* is able to ensure constraints. As the actuators capabilities are limited, the modified reference lead to a degraded attitude tracking. Attitude reference is then longer to be reached, but without any loss of stability or sloshing torque estimation performance due to actuators saturations.

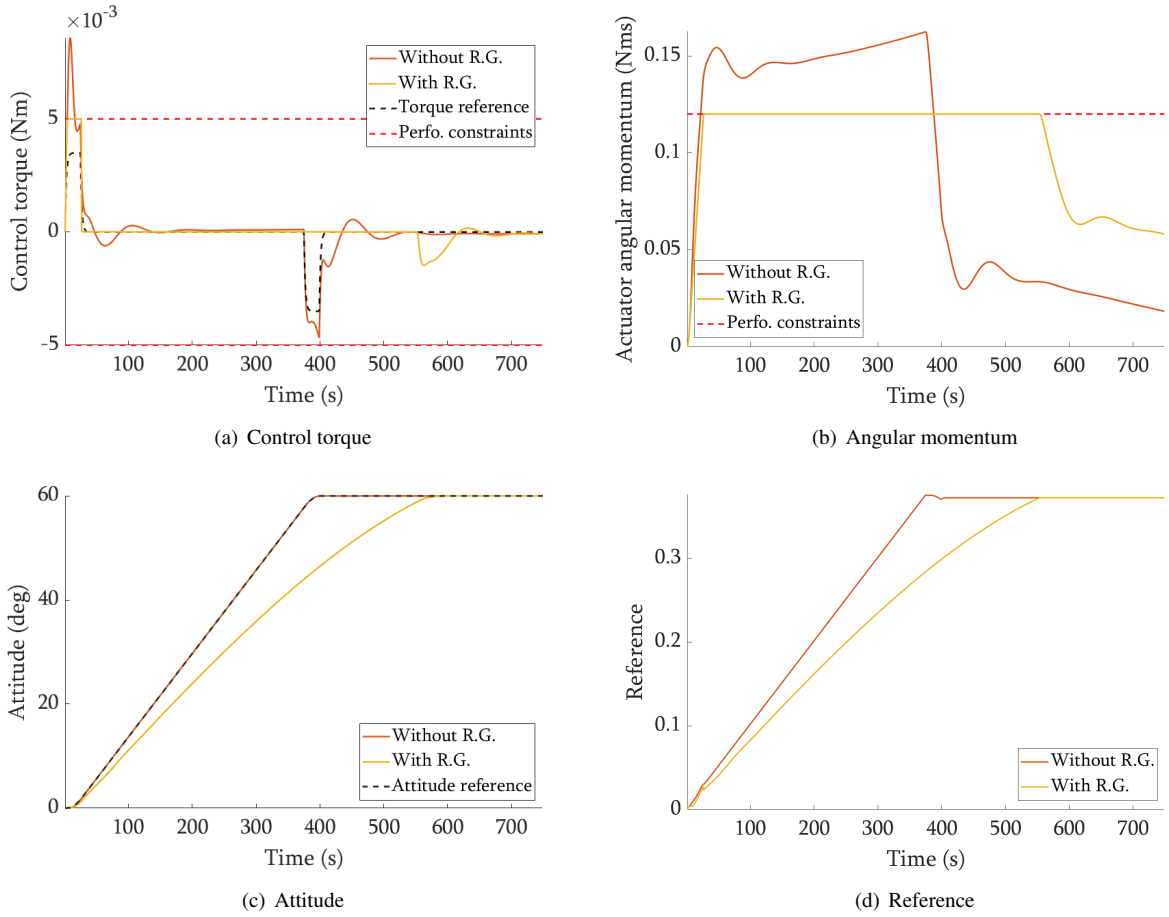

(a) Control torque

(b) Angular momentum

(c) Attitude

(d) Reference

Figure 11: Reference governor performances

6. Conclusion

In this paper we have presented a complete procedure to handle sloshing disturbances in spacecraft during attitude maneuvers. Results have been recalled concerning a new way to model the propellant-filled spacecraft as an uncertain LPV system with a compensation scheme based on the design of a robust observer by means of multi-model $\mathcal{H}_\infty$ framework. This technique has been proven to guarantee quadratic stability over the parametric domain. This paper present an enhancement of the compensation scheme by the design of a *reference governor* to handle actuators saturations despite adverse initial conditions. As attitude tracking error was considerably reduced to acceptable values, the use of such attitude control systems with an efficient sloshing dynamics mitigation could allow to reduce tank complexity

and mass, and improve mission availability. Future work will focus on the extension to three-axis maneuvers and the validation of this compensation scheme with a coupled CFD-Matlab simulator.

7. Acknowledgments

This study was co-funded by ONERA, The French Aerospace Lab, and CNES, The French Space Agency.

References

[1] H Norman Abramson, Helmut F Bauer, George W Brooks, and Wen-Hwa Chu. The dynamic behavior of liquids in moving containers, with applications to space vehicle technology (nasa-sp-106). Technical report, 1966.

[2] David Angeli, Alessandro Casavola, and Edoardo Mosca. Command governors for constrained nonlinear systems: direct nonlinear vs. linearization-based strategies. *International Journal of Robust and Nonlinear Control: IFAC-Affiliated Journal*, 9(10):677–699, 1999.

[3] P. Apkarian and D. Noll. Nonsmooth $\mathcal{H}_\infty$ synthesis. *IEEE Trans. on Automatic Control*, 51(1):71–86, 2006.

[4] Pierre Apkarian, Pascal Gahinet, and Craig Buhr. Multi-model, multi-objective tuning of fixed-structure controllers. In *Proceedings of ECC 2014*, pages 856–861, 2014.

[5] Hamid Alemi Ardakani and Thomas J Bridges. Shallow-water sloshing in vessels undergoing prescribed rigid-body motion in three dimensions. *Journal of Fluid Mechanics*, 667:474–519, 2011.

[6] Robert L Berry and James R Tegart. Experimental study of transient liquid motion in orbiting spacecraft (nasa-cr-144003). Technical report, 1975.

[7] J-M Biannic and Pierre Apkarian. Missile autopilot design via a modified lpv synthesis technique. *Aerospace Science and Technology*, 3(3):153–160, 1999.

[8] Jean-Marc Biannic, Clement Roos, and Christelle Pittet. Linear parameter varying analysis of switched controllers for attitude control systems. *Journal of Guidance, Control, and Dynamics*, 34(5):1561–1567, 2011.

[9] Anthony Bourdelle, Jean-Marc Biannic, et al. Propellant sloshing torque h-infinity based observer design for enhanced attitude control. In *ACA 2019 Proc.*, 2019.

[10] Anthony Bourdelle, Laurent Burlion, Jean-Marc Biannic, et al. Towards new control design oriented models for fuel sloshing in observation spacecraft. In *AIAA Scitech 2019 Forum*, page 0115, 2019.

[11] Thomas Breinlinger, Pit Polfer, Adham Hashibon, and Torsten Kraft. Surface tension and wetting effects with smoothed particle hydrodynamics. *Journal of Computational Physics*, 243:14–27, 2013.

[12] Flávio Luiz Cardoso-Ribeiro, Denis Matignon, and Valérie Pommier-Budinger. Control design for a coupled fluid-structure system with piezoelectric actuators. *Proceedings of the 3rd CEAS EuroGNC*, pages 13–15, 2015.

[13] Luigi Chisci, Paola Falugi, and Giovanni Zappa. Predictive tracking control of constrained nonlinear systems. *IEE Proceedings-Control Theory and Applications*, 152(3):309–316, 2005.

[14] Luiz Carlos Gadelha de Souza and Alain G de Souza. Satellite attitude control system design considering the fuel slosh dynamics. *Shock and Vibration*, 2014, 2014.

[15] Franklin T Dodge. Engineering study of flexible baffles for slosh suppression (nasa cr-1880). Technical report, 1971.

[16] Vincent Duindam, Alessandro Macchelli, Stefano Stramigioli, and Herman Bruyninckx. *Modeling and control of complex physical systems: the port-Hamiltonian approach*. Springer, 2009.

[17] P. J. Enright and E. C . Wong. Propellant slosh models for the cassini spacecraft. Technical report, Jet Propulsion Laboratory, Caltech, 1994.

[18] Jaime Rubio Hervas and Mahmut Reyhanoglu. Control of a spacecraft with time-varying propellant slosh parameters. In *ICCAS 2012*, pages 1621–1626. IEEE, 2012.

[19] Eric J Hoffman, WL Ebert, MD Femiano, HR Freeman, CJ Gay, CP Jones, PJ Luers, and JG Palmer. The near rendezvous burn anomaly of december 1998. *Applied Physics Laboratory, Johns Hopkins University*, 1999.

[20] Raouf A Ibrahim. *Liquid sloshing dynamics: theory and applications*. Cambridge University Press, 2005.

[21] Ilya Kolmanovsky, Emanuele Garone, and Stefano Di Cairano. Reference and command governors: A tutorial on their theory and automotive applications. In *American Control Conference (ACC), 2014*, pages 226–241. IEEE, 2014.

[22] Mathieu Lepilliez, Elena Roxana Popescu, Frederic Gibou, and Sébastien Tanguy. On two-phase flow solvers in irregular domains with contact line. *Journal of Computational Physics*, 321:1217–1251, 2016.

[23] Xiangdong Liu, Xing Xin, Zhen Li, Zhen Chen, and Yongzhi Sheng. Near minimum-time feedback attitude control with multiple saturation constraints for agile satellites. *Chinese Journal of Aeronautics*, 29(3):722–737, 2016.

[24] Leonardo Mazzini. *Flexible Spacecraft Dynamics, Control and Guidance*. Springer, 2015.

[25] Jean Mignot et al. Fluid dynamics in space experiment. IAC, 2017.

[26] Nicolas Petit and Pierre Rouchon. Dynamics and solutions to some control problems for water-tank systems. *IEEE Transactions on Automatic Control*, 47(4):594–609, 2002.

[27] C Pittet and D Arzelier. Demeter: A benchmark for robust analysis and control of the attitude of flexible micro satellites. *IFAC Proceedings Vol.*, 39(9):661–666, 2006.

[28] André Preumont. *Vibration control of active structures*, volume 2. Springer, 1997.

[29] JJM Prins. *SLOSHSAT FLEVO - Description of the mini satellite*. Citeseer, 2000.

[30] Mahmut Reyhanoglu and Jaime Rubio Hervas. Nonlinear control of a spacecraft with multiple fuel slosh modes. In *CDC-ECC*, pages 6192–6197. IEEE, 2011.

[31] Ye Somov, S Butyrin, S Somov, and C Hajiyev. Attitude guidance, navigation and control of land-survey mini-satellites. *IFAC OnLine*, 48(9):222–227, 2015.

[32] Pantelis Sopasakis, Daniele Bernardini, Hans Strauch, Samir Bennani, and Alberto Bemporad. Sloshing-aware attitude control of impulsively actuated spacecraft. In *2015 European Control Conference (ECC)*, pages 1376–1381. IEEE, 2015.

[33] Walter Tam, Katherine Dommer, Samuel Wiley, Larry Mosher, and David Persons. Design and manufacture of the messenger propellant tank assembly. In *38th AIAA/ASME/SAE/ASEE Joint Propulsion Conference & Exhibit*, page 4139, 2002.

[34] Arthur EP Veldman, Jeroen Gerrits, Roel Luppes, Joop A Helder, and JPB Vreeburg. The numerical simulation of liquid sloshing on board spacecraft. *Journal of Computational Physics*, 224(1):82–99, 2007.

[35] Damien Violeau. *Fluid mechanics and the SPH method: theory and applications*. Oxford University Press, 2012.

[36] Jan Vreeburg and David Chato. Models for liquid impact onboard sloshsat flevo. In *Space 2000 Conference and Exposition*, page 5152, 2000.

[37] Ken'ichi Yano and Kazuhiko Terashima. Robust liquid container transfer control for complete sloshing suppression. *IEEE Trans. on Control Systems Tech.*, 9(3):483–493, 2001.